Ratiometric Two-Photon Fluorescent Probes for Mitochondria! Hydrogen Sulfide in Living Cells

ARTICLE *in* THE JOURNAL OF ORGANIC CHEMISTRY · SEPTEMBER 2014

Impact Factor: 4.72 · DOI: 10.1021/jo5014838 · Source: PubMed

4 AUTHORS, INCLUDING:

Qinhua Song
University of Science and Technology of China
65 PUBLICATIONS **599** CITATIONS

SEE PROFILE

JOC The Journal of Organic Chemistry

Article

pubs.acs.org/joc

Ratiometric Two-Photon Fluorescent Probes for Mitochondrial Hydrogen Sulfide in Living Cells

Xiu-Ling Liu,[†] Xiao-Jiao Du,[‡] Chun-Guang Dai,[†] and Qin-Hua Song*,[†]

[†]Department of Chemistry, University of Science and Technology of China, Hefei 230026, P. R. China

[‡]School of Life Sciences, University of Science and Technology of China, Hefei 230027, P. R. China

Supporting Information

ABSTRACT: Hydrogen sulfide (H_2S) is an important signaling molecule with diverse biological roles. Various fluorescent probes for H_2S with biological application have been developed. However, two-photon ratiometric imaging of mitochondrial H_2S is scarce. In this paper, we report two ratiometric two-photon probes, AcHS-1 and AcHS-2, which employ 4-amino-1,8-naphthalimide as the fluorophore and 4-azidobenzyl carbamate as the H_2S response site. These probes exhibit high selectivity toward H_2S over biothiols and other reactive species, low detection limits of 50−85 nM, low cytotoxicity, and high stability under physiological conditions. Furthermore, through cell imaging with one-photon and two-photon microscopy, MCF-7 cells incubated with two probes show a marked change in emission color from blue to green in response to H_2S. Cell images costraining with a mitochondrial dye reveal that AcHS-2 is a mitochondria-specific two-photon probe for H_2S. These results show that AcHS-2 may find useful applications in biological research such as tracking mitochondrial H_2S in living biological specimens.

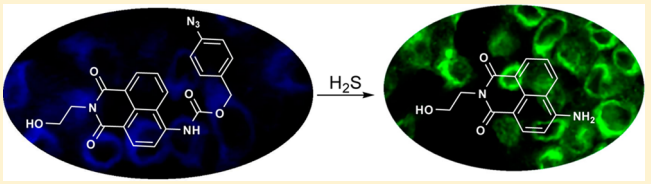

INTRODUCTION

Hydrogen sulfide (H_2S) is a ubiquitous gaseous signaling molecule generated predominately from cysteine by two pyridoxal-5′-phosphate-dependent enzymes, cystathionine-β-synthase and cystathionine-γ-lyase, as well as by 3-mercapto-sulfurtransferase, in the cytosols and mitochondria of mammalian cells in relatively high concentration (10−100 μM).[1,2] The significance of endogenous H_2S has been recognized in a number of physiological and pathological processes.[3,4] H_2S plays critical roles in regulating intracellular redox status and other fundational signaling processes involved in human health and disease.[1,5] Mitochondrial H_2S has been shown to exert protective effects in oxidative stress leading to dysfunction and cell death,[6−8] and has become the focus of many research endeavors, including pharmacotherapeutic manipulation.[9]

To detect H_2S in solutions and cells, a number of fluorescent probes[10] have been designed on the basis of reactions of H_2S as a reductant to reduce azide or nitro group on masked fluorophore[11] or as a nucleophile to attack activated electrophiles,[12] precipitate metal salts,[13] or others.[14] Most of them are turn-on fluorescent probes, which are difficult to give quantitative information on the H_2S concentration, since molecular emission intensity can be distinctly affected by photobleaching, microenvironments, and local probe concentration. Therefore, ratiometric probes for H_2S are highly appealing owing to their ability in quantitative tracking. So far, a few ratiometric H_2S probes have been reported.[11d,l,12a,b,14b−e] In addition, under one-photon excitation, short excitation wavelengths (<500 nm) limit applications of these probes with regard to deep-tissue imaging due to the shallow penetration depth (<100 μm). An attractive approach for the detection of H_2S in organelles deep inside the tissues is through the use of two-photon microscopy (TPM), which employs near-IR photons as the excitation source, and it offers many advantages, including greater penetration depth (>500 μm), localization of the excitation, and longer observation times.

Furthermore, selective tracking of H_2S in an organelle such as mitochondria is crucial to elucidate the complex contributions of H_2S in the physiological and pathological processes. However, five ratiometric fluorescent probes for mitochondrial H_2S have been reported,[11l,12a,b,14d,e] and only one case[11l] is a two-photon probe. Therefore, this is still a strong need and requires challenging work to develop new ratiometric two-photon probes for mitochondrial H_2S.

In this work, we developed two ratiometric fluorescent probes, AcHS-1 and AcHS-2, for detection of H_2S. Moreover, we demonstrated that AcHS-2 is a new mitochondria-specific probe for H_2S, and mitochondrial images can be achieved under both one-photon and two-photon excitations.

RESULTS AND DISCUSSION

1. Design and Synthesis of Probes. 4-Amino-1,8-naphthalimide with intramolecular charge transfer (ICT) has been used as a fluorophore in H_2S fluorescent probes,[11e,g,12k] but all these probes are the turn-on mode, as shown in Scheme 1. By modifying an ICT-state fluorophore to change the ICT property, the modified fluorophore could display a ratiometric spectral variation. If certain molecules such as H_2S can induce a

Received: July 3, 2014

   dx.doi.org/10.1021/jo5014838 | J. Org. Chem. XXXX, XXX, XXX−XXX

Scheme 1. Reported Probes with a Turn-On Response Mode[11e,g]

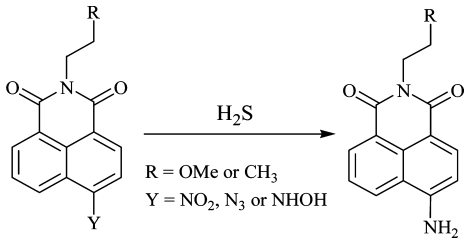

sensing reaction to remove this modifying group, the modified fluorophore would become a ratiometric two-photon fluorescent probe for the molecule. Based on this design strategy of ratiometric two-photon fluorescent probes, we designed two ratiometric probes for H_2S, using 4-amino-1,8-naphthalimide as the fluorophore and 4-azidobenzyl carbamate as a H_2S response site, shown in Scheme 2. As the azide is reduced to amine, probes may undergo a cleavage of the carbamate and release of the amino group. The 4-amino-1,8-naphthalimides with ICT states have large two-photon absorption cross sections.[15] Through introducing an electron-withdrawing carbamate group to convert the 4-amino donor into a weak donor, the ICT effect of the fluorophore is weakened to result in a blue-shift of fluorescence. On this basis that the thiolate-triggered reaction with the azide group would cleave the carbamate linkage and liberate the amine group,[16,17] we expect that a similar cleavage and release occurs for the new probes in the presence of H_2S.

The synthetic procedure for probes AcHS-1 and AcHS-2 is outlined in Scheme 3. Using 4-azidophenylmethyl bromide as a starting material, 4-azidophenylmethanol (**5**)[18] was prepared. *n*-Butylamine or aminoethanol was quickly added to a cloudy solution of 4-nitro-1,8-naphthalic anhydride[19] in ethanol. After being refluxed for 6 h under N_2, the solution was filtered, washed, and purified to give compound **6a**[20] or **6b**.[21] A stirred cloudy solution of **6a** or **6b** in ethanol was added to the solution of $SnCl_2$ in concentrated hydrochloric acid at room temperature to afford compound **3**[20] or compound **4**.[21] A mixture of **3** or **4** and DMAP in toluene was added to a solution of triphosgene in toluene, heated to reflux for 3 h, diluted with CH_2Cl_2, and filtered. To the filtrate was added compound **5**, stirred at room temperature for 3 h, and purified to give target products AcHS-1 and AcHS-2.

2. Spectral Response to H_2S in Aqueous Solutions. H_2S is a weak acid in aqueous solutions (pK_{a1} = 7.04, pK_{a2} = 11.96),[22] equilibrating mainly with HS^- at physiological pH. For example, at pH 7.4 and temperature of 37 °C, 18.5% of free hydrogen sulfide exists as H_2S molecule and the remainder is almost all hydrosulfide anion (HS^-) with a negligible contribution of S^{2-}.[23] As the ion distribution of Na_2S is the same with that of H_2S in a neutral buffer solution, Na_2S was employed to replace H_2S in this work.

Parts a and c of Figure 1 show time-dependent UV/vis absorption spectra of 10 μM AcHS-1 and 10 μM AcHS-2 in the presence of 1 mM Na_2S, respectively. The absorption band in the range of 400−500 nm appears and increases, accompanying the decrease in the absorption peak at 370 nm. This change results in an isosbestic point at 400 nm, indicating the sensing reaction is a single transformation. The final absorption spectra show a larger red shift of 65 nm for AcHS-1 and 63 nm for AcHS-2 over those[11l] of two probes reported (25 nm for SHS-M1 and 40 nm for SHS-M2). The color change of the solution from colorless to yellow can be observed by the naked eye (inset of Figure 1a).

The time-dependent fluorescent response of AcHS-1 or AcHS-2 to H_2S was also observed. The fluorescence spectra of AcHS-1 and AcHS-2 have a wide emission band (400−600 nm) with a peak at 468 nm for both AcHS-1 and for AcHS-2. With addition of Na_2S, the cleavage reaction of AcHS-1 or AcHS-2 would trigger and release the green fluorescent **3** or **4** with a stronger ICT-state emission ($\Phi_f(\mathbf{3})$ = 0.13, $\Phi_f(\mathbf{4})$ = 0.12 listed in Table 1). Consequently, the fluorescence emission intensity in the short wavelength region gradually decreases, accompanying appearance of a new emission band (475−650 nm) with a peak at 530 nm, exhibiting a ratiometric change with a large red-shift over 62 nm for both AcHS-1 and AcHS-2 as shown in Figure 1b,d. Fluorescence photos of AcHS-1 solutions without and with Na_2S are shown in the inset of Figure 1b. The ratio of F_{530}/F_{468} increases from 0.35, 0.28 to 3.37, 2.02 for AcHS-1 and AHS-2, respectively, after incubation for 2 h.

Two-photon absorption cross sections (δ) were obtained by determining the two-photon absorption action spectra of probes and their sensing products **3** and **4**, listed in Table 1. The δ_{max} values for AcHS-1 and AcHS-2 were 152 and 119

Scheme 2. Proposed Sensing Mechanism of Probes, AcHS-1 and AcHS-2

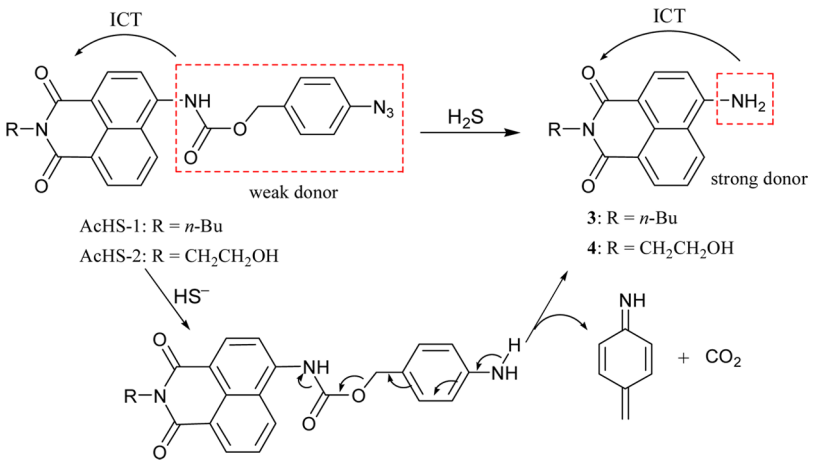

dx.doi.org/10.1021/jo5014838 | J. Org. Chem. XXXX, XXX, XXX−XXX

Scheme 3. Synthetic Route of Probes AcHS-1 and AcHS-2

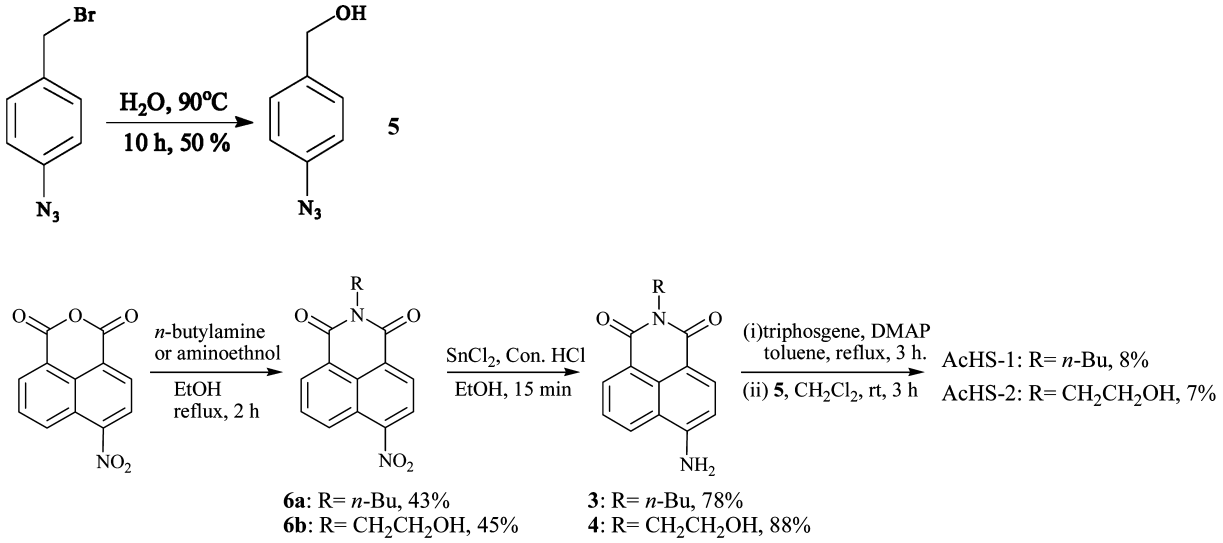

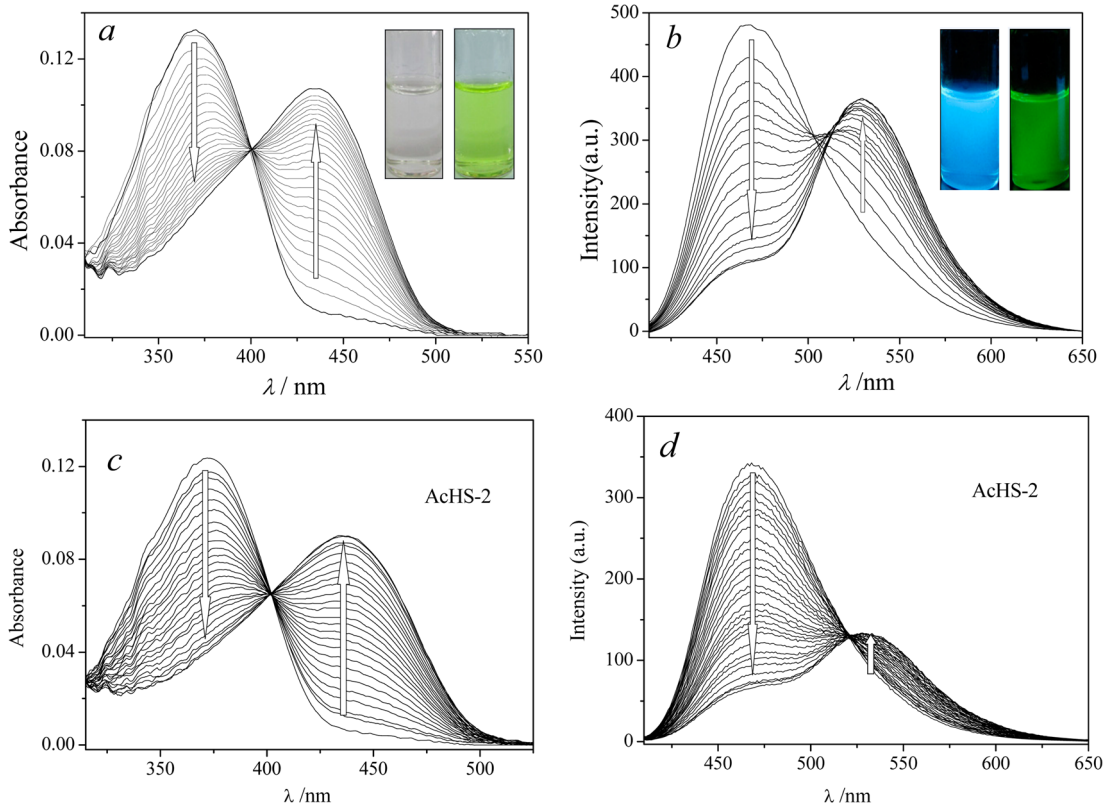

Figure 1. Time-dependent UV/vis absorption (a, c) and fluorescence spectra (b, d) of 10 μm AcHS-1 or AcHS-2 in EtOH/PBS (v/v1:4, pH 7.0) response toward Na_2S (1 mM), respectively, excitation at 410 nm. Insets in (a) and (b): photograph for the solution color and the fluorescent changes of AcHS-1 without and with Na_2S in the buffer solution, respectively.

GM, respectively, and lower than those of **3** and **4** (207 and 218 GM, respectively). The higher two-photon absorption cross-sections for **3** and **4** over the probes can be attributed to their enhanced donor, 4-amino group.

3. Sensing Mechanism. To further confirm the validity of the proposed sensing mechanism, the sensing reaction of AcHS-1 to Na_2S in DMSO-d_6 was analyzed by means of NMR spectroscopy, with partial ^{1}H NMR spectra shown in Figure 2. As shown in Figure 2a, a characteristic single peak at 5.48 ppm was assigned to the proton (H^8) of AcHS-1, and the single peak was not observed from the ^{1}H NMR spectrum of the reaction mixture of AcHS-1 and Na_2S (Figure 2b). In this field region, most of the emerging peaks for ^{1}H NMR spectrum of the reaction mixture match with those of compound **3**. Hence, the sensing reaction of AcHS-1 with Na_2S could occur via the cleavage of azido-based carbonate moiety and release of **3**. Furthermore, the main H_2S-induced product is confirmed to be compound **3** by coinjection HPLC analysis. As shown in Figure 3, with increasing reaction time, the chromatogram peak at 19.5

dx.doi.org/10.1021/jo5014838 | J. Org. Chem. XXXX, XXX, XXX–XXX

Table 1. Photophysical Data for AcHS-1, AcHS-2, 3, and 4[a]

compd	$\lambda_{abs}(10^{-4}\varepsilon)$[b]	λ_{fl}[c]	Φ[d]	λ_{max}[e]	δ_{max}[f]
AcHS-1	370 (1.34)	468	0.15	740	152
3	435 (1.20)	530	0.13	820	207
AcHS-2	373 (1.34)	468	0.10	730	119
4	436 (1.18)	530	0.12	800	218

[a]Measurements were performed in EtOH/PBS (v/v1:4, 100 mM, pH 7.0), unless otherwise noted. [b]λ_{max} of the one-photon absorption spectra in nm. The values in parentheses are molar extinction coefficients in M^{-1} cm^{-1}. [c]Fluorescence maxima. [d]Fluorescence quantum yields, ± 10%. [e]λ_{max} of the two-photon absorption action spectra in nm, measured in acetonitrile. [f]Peak two-photon absorption action cross sections in GM (1 GM = 10^{-50} m^4 s $photon^{-1}$), ± 10%, measured in acetonitrile.

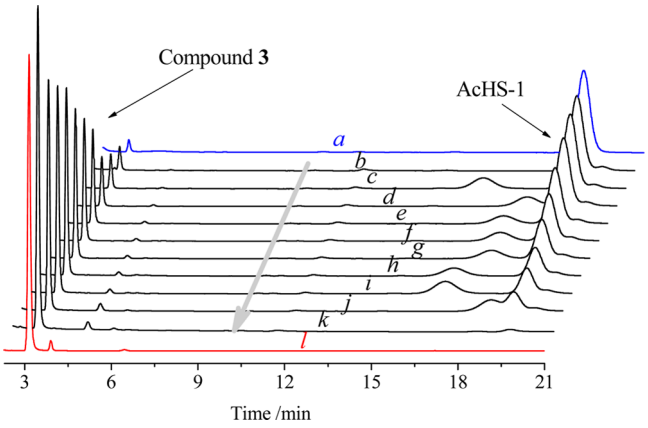

Figure 3. Time-dependent HPLC profiles of AcHS-1 (10 μM) in the presence of Na_2S (1 mM) in methanol/water (1:1, v/v). The eluent is a methanol/water solvent mixture (80:20, v/v), monitored at 254 nm (a, 0 min; b, 5 min; c, 10 min; d–j, interval of 20 min; k, 4 h; l, neat compound **3**). Retention times: 3.2 min (product **3**), 19.5 min (AcHS-1).

min of AcHS-1 decreases with a simultaneous increase for a new peak at 3.2 min, which is assigned to compound **3**.

4. Sensitivity and Selectivity. *Detection Limits.* The fluorescence spectra of 0.2 μM AcHS-1 in EtOH/PBS (v/v1:4, pH 7.0) in the presence of various concentrations of Na_2S from 0 to 6 μM were collected and are shown in Figure S1 (Supporting Information). A linear regression curve was then fitted according to the ratio of fluorescence intensity at F_{530}/F_{465} in the range of [Na_2S] from 0 to 6 μM. The detection limit ($3N/k$) was determined to be 0.05 μM, where N is the standard deviation of the intercept and k is the slope of the fitting straight line in the inset of Figure S1 (Supporting Information). Similarly, the detection limit of AcHS-2 was obtained, 0.085 μM (Figure S2, Supporting Information).

Selectivity. The selectivity of probes was determined for H_2S over other biologically relevant species, including reactive sulfide (cysteine (Cys), glutathione (GSH), SCN^-), reductants ($S_2O_3^{2-}$, SO_3^{2-}, ascribic acid (Vc), $S_2O_4^{2-}$), reactive oxygen (HClO, H_2O_2, *t*-BuOOH), nitrogen species (NO_2^-), and metal ions (Ca^{2+}, Na^+, K^+). Both AcHS-1 and AcHS-2 displayed a marked response for H_2S over other biological relevant species. As shown in Figure 4, pronounced fluorescence changes were observed from the solution with H_2S, and no significant change occurred for solutions with other analytes. The fluorescence intensity ratios (F_{530}/F_{468}) for Na_2S over other analytes were 8–17-fold for AcHS-1 and 5–7-fold for AcHS-2. Meanwhile, the naked-eye color of probe solutions changed from colorless to yellow, and the emission color from blue to green only in the presence of Na_2S (inset of Figure 4left).

5. pH Effect on Fluorescent Response and Stability of Probes. To examine the pH-dependent fluorescent response, fluorescence intensities of the sensing reaction in different solutions (pH 2.0–10.0) were measured (Figure 5a). The fluorescence spectra of probes AcHS-1 and AcHS-2 were recorded at various pH solutions (EtOH/PBS (v/v1:4). The pH-dependence response was estimated by the fluorescence intensity ratio at F_{530}/F_{468} under excitation at 410 nm. Under neutral or alkaline conditions (pH > 6), probes AcHS-1 and AcHS-2 can respond to H_2S with a remarkable fluorescence

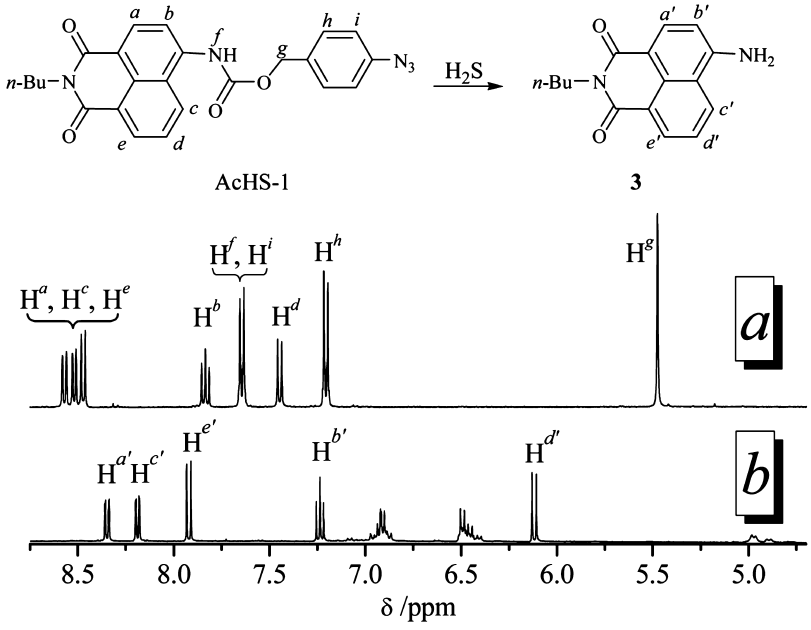

Figure 2. Partial ^{1}H NMR (400 MHz) spectra of AcHS-1 (a), AcHS-1 and Na_2S (molar ratio 1:10) in DMSO-d_6 (b).

dx.doi.org/10.1021/jo5014838 | J. Org. Chem. XXXX, XXX, XXX–XXX

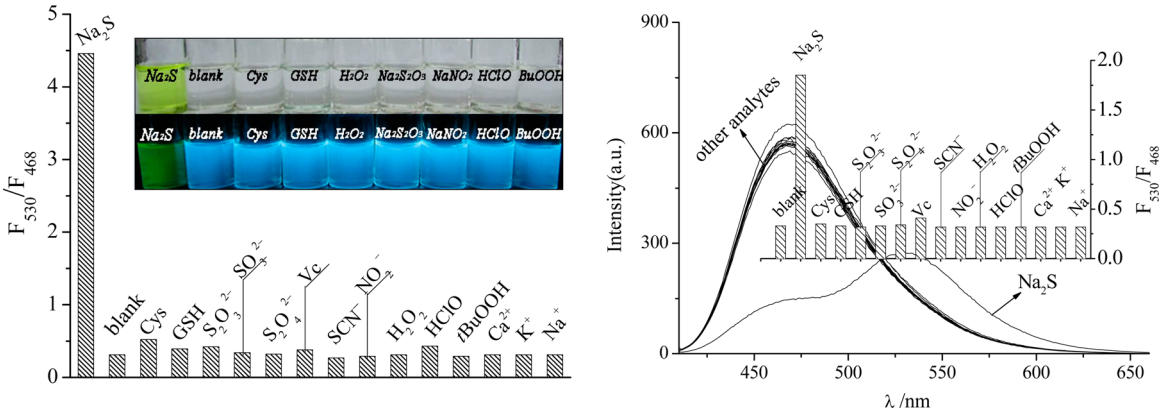

Figure 4. Left: Fluorescence responses of AcHS-1 (10 μM) to various analytes (1 mM) at F_{530}/F_{468} in EtOH/PBS (v/v1:4, pH 7.0). Inset: photos of naked-eye and fluorescent responses of AcHS-1 to various analytes. Right: fluorescence spectra of AcHS-2 (10 μM) in the presence of various analytes (1 mM) in the buffer solution. Inset: the corresponding fluorescence response, under excitation at 400 nm, incubation for 2 h.

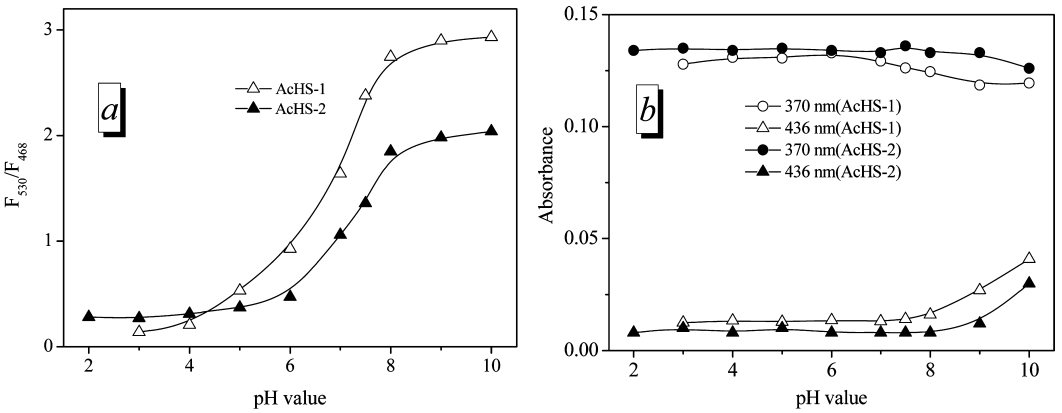

Figure 5. (a) Plot of the ratio of F_{530}/F_{468} for AcHS-1 (10 μM) and AcHS-2 (10 μM) vs pH value in the presence of 1 mM Na_2S. (b) Absorbance at 370 and 436 nm of 10 μM AcHS-1 and AcHS-2, in different pH solutions, incubation for 2 h.

change, while no obvious response was observed in acidic solutions (pH < 5).

For the pH effect on the stability of the probes, UV/vis absorption spectra of AcHS-1 and AcHS-2 in various solutions from pH 2 to 10 were recorded, respectively (Figure 5b). The stability of probes AcHS-1 and AcHS-2 were estimated by measuring the absorbance at 370 mn for absorption peak of the probes and 436 nm for absorption peak of compound **3** in various pH solutions (Figure 5b). As shown in Figure 5b, no significant change at the two wavelengths, 370 and 436 nm, was observed at pH 2−8. This indicates that the probes are stable in pH 2−8 solutions. In addition, the stability of probes under the physiological condition was also estimated by tracking their UV/vis absorption spectra in a PBS buffer (pH 7.4) for 10 h (Figure S3, Supporting Information). Their absorption spectra display no significant change. These results show that AcHS-1 and AcHS-2 not only can detect H_2S but also are considerably more stable under physiological conditions (pH 6−8).

6. Fluorescence Imaging of Living Cells. *Cell Toxicity of Probes.* In order to detect H_2S in living MCF-7 cells, a MTT experiment was carried out to assess the cytotoxicity of the probes. In the MTT assays, MCF-7 cells were dealt with probes in different concentrations from 5 to 20 μM for 24 h. The results show that the probes have low toxicity to cultured cells under the experimental conditions (Figure 6) and the cell viability is 93% and 89% for AcHS-1 and AcHS-2 at 5 μM, respectively.

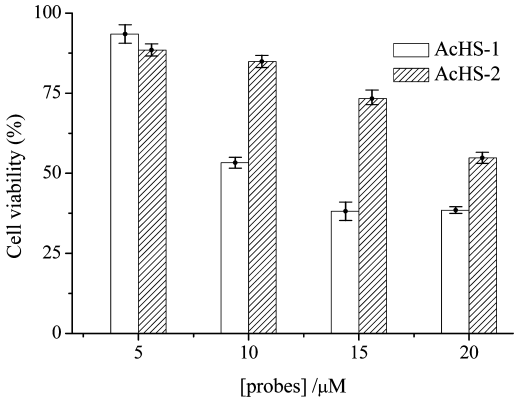

Figure 6. MTT assay of MCF-7 cells in the presence of different concentrations of probes.

Fluorescent Imaging of Cells. The MCF-7 cells were placed in a 96-well plate and treated with 5 μM AcHS-1 or AcHS-2 for 1 h, and then the cells in one well were incubated with 0.5 mM Na_2S for an additional 1 h. Two types of cells were washed with PBS three times for confocal fluorescence microscopy (Figures 7 and 8). As shown in Figure 7, cells incubated alone with AcHS-1 display blue emission collected from the blue channel (408−500 nm), and cells costained by AcHS-1 and Na_2S emit green fluorescence collected from the green channel (500−650 nm) under one-photon excitation of 405 nm. Upon two-

dx.doi.org/10.1021/jo5014838 | J. Org. Chem. XXXX, XXX, XXX−XXX

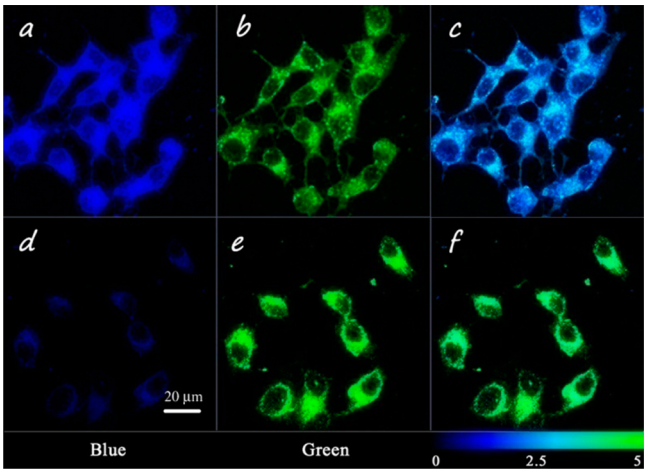

Figure 7. Confocal fluorescence images of MCF-7 cells incubated with 5 μM AHS-1 for 1 h (a–c) and then 0.5 mM Na_2S for 1 h (d–f). Images were acquired using 405 nm excitation and emission channels of 408–500 nm (blue) and 500–650 nm (green). Cells shown are representative images from replicate experiments (n = 3).

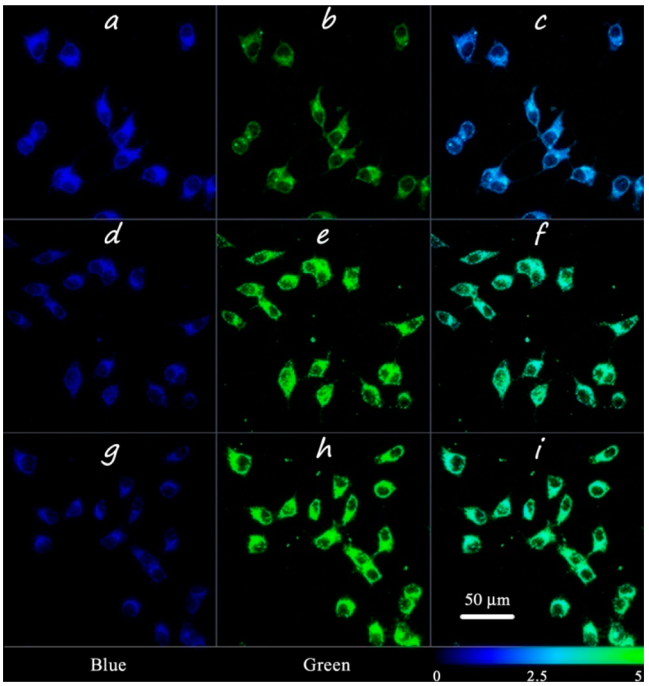

Figure 8. Confocal fluorescence images of MCF-7 cells incubated with 5 μM AHS-2 for 1 h (a–c) and then 0.5 mM Na_2S for 1 h, under 405 nm excitation (d–f) and 800 nm excitation (g–i). Images were acquired with emission channels of 408–500 nm (blue) and 500–650 nm (green). Cells shown are representative images from replicate experiments (n = 3).

photon excitation at 750 nm, cells stained alone with AcHS-1 emitted similar fluorescence, shown in Figure S4 (Supporting Information).

Similarly, cells stained by AcHS-2 with and without Na_2S emit different-color fluorescence (Figure 8a–f). Moreover, upon two-photon excitation at 750 nm for cells stained alone with AcHS-2 as shown in Figure S4 (Supporting Information) and 800 nm for cells costained by AcHS-2 and Na_2S (Figure 8g–i), confocal fluorescence microscopy collects similar emissions from the two channels. These results show that AcHS-2 can detect H_2S in live cells by cellular imaging under both one-photon and two-photon excitation.

From the ratiometric fluorescence images shown in Figures 7 and 8, the values of F_{green}/F_{blue}, the ratio of the relative emission intensity of 500–650 nm (green) and 408–500 nm (blue), showed large changes for systems between with and without Na_2S (Figure 9). The values of F_{green}/F_{blue} for MCF-7 cells stained alone with AcHS-1 and AcHS-2 were 0.31 and 0.38, and the values for the cells incubated with additional Na_2S increased to 3.9 and 2.9, respectively. This indicates that two probes can serve as ratiometric fluorescent probes for H_2S in cells.

The cell images above show that the probes could localize at mitochondria. To further investigate the mitochondria localization of AcHS-2, a commercially available mitochondrial dye (MitoTracker Red CMXRos)[24] was employed for a colocalization study. MCF-7 cells were stained with AcHS-2 and the MitoTracker in succession and observed under the confocal fluorescence microscopy by one- and two-photon images. As shown in Figure 10, the green-channel images for AcHS-2 with and without Na_2S merged well with the red-channel images for MitoTracker dye under one-photon excitation (Figure 10d, h). The colocalization assay with the mitochondrial dye and AcHS-2 revealed that fluorescence of AcHS-2 was colocalized with that of the mitochondrial dye, and the overlap coefficients were 0.79 for the cells without Na_2S (Figure 10d) and 0.71 for the cells with Na_2S (Figure 10h). Upon one- and two-photon excitation at 375 and 750 nm, confocal images of MCF-7 cells costained by AcHS-2 and anther mitochondrial specific dye MitoTracker Deep Red FM[24] displayed excellent overlap between the green-channel images for AcHS-2 and the red-channel images for the MitoTracker dye under one-photon excitation (Figure S5, Supporting Information). The overlap coefficients between the green channel and the red channel were 0.80 for one-photon image (Figure S5d, Supporting Information), 0.87 for two-photon image (Figure S5h, Supporting Information). The high overlap coefficients indicate that AcHS-2 can accumulate in the mitochondria.

It is well-known that the commercial dyes for mitochondria are cationic and can accumulate in the mitochondria due to the negatively charged surface of the mitochondrial membrane. In this work, however, two probes are electroneutral, and the difference in structures is *N*-*n*-butyl for AcHS-1 and *N*-(2-hydroxyethyl) for AcHS-2. By comparing cell images of two probes, we found that all images of the cells stained with AcHS-2 were brighter than those stained with AcHS-1. Hence, we inferred that the hydrogen bonds formed between the hydroxyl group (and 4-amino) with mitochondrial membrane may be the reason why the probes, especially AcHS-2, accumulate in the mitochondria.

CONCLUSION

In summary, we developed two ratiometric two-photon fluorescent probes based on an ICT-state fluorophore, 4-amino-1,8-naphthalimide. By modifying the fluorophore with an electron-withdrawing group, 4-azidophenyl methoxy carbonyl, to convert the amino group into a weak donor, also as the site of the sensing reaction to H_2S, the resulting probe molecules display a new ICT property, affording ratiometric spectral changes and achieving two-photon excitation. The two fluorescent probes can be used for specific ratiometric sensing of H_2S upon both one-photon and two-photon excitation. The study provided a design strategy of ratiometric two-photon fluorescent probes. Furthermore, cell-imaging experiments

dx.doi.org/10.1021/jo5014838 | J. Org. Chem. XXXX, XXX, XXX–XXX

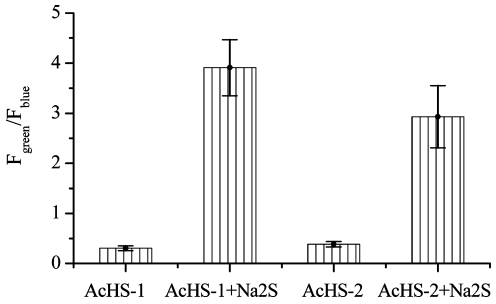

	F_{green}/F_{blue}
AcHS-1	0.31 ± 0.048
AcHS-1+Na$_2$S	3.9 ± 0.56
AcHS-2	0.38 ± 0.055
AcHS-2+Na2S	2.9 ± 0.62

Figure 9. Average intensity ratios (F_{green}/F_{blue}) for AcHS-1, AcHS-1/Na_2S (Figure 7cf), AcHS-2, and AcHS-2/Na_2S (Figure 8cf).

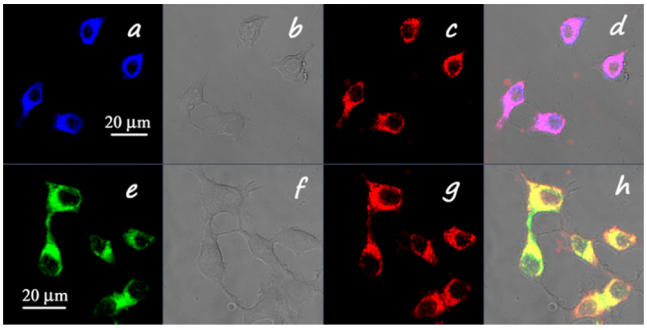

Figure 10. Confocal fluorescence images of MCF-7 cells costained by AcHS-2 (5 μM, 1 h) and MitoTracker Red CMXRos (0.5 μM, 30 min) without (a–d) and with 0.5 mM Na_2S (e–h): (a, e) fluorescence images obtained with band paths of 408–500 nm for cells incubated by only AcHS-2 and 500–650 nm for incubated by AcHS-2 and Na_2S, upon excitation of AcHS-2 at 405 nm; (b, f) bright-field images; (c, g) images from a band path of 600–705 nm; (d, h) merged images of (a), (b) and (c) or (e), (f) and (g).

reveal that AcHS-2 is a new mitochondria-specific and emission-ratiometric two-photon probe for H_2S. The new probe is promising to be utilized in a variety of chemical and biological applications.

EXPERIMENTAL SECTION

Instrumentation and Methods. ^1H and ^{13}C NMR spectra were recorded on an NMR spectrometer operating at 400 or 300 and 75 MHz, respectively. FT-IR spectra were carried out with an infrared spectrometer. High-resolution mass spectrometry data were obtained with a FTMS spectrometer or a LC–TOF MS spectrometer. UV–vis absorption spectra and fluorescence spectra were recorded at room temperature on a UV/vis spectrometer and a sprectrofluorophotometer, respectively. The reaction mixtures of the probe with H_2S were analyzed by a HPLC with a C-18 reversed-phase column.

General Procedure for Spectral Measurements. Sample solutions of AcHS-1 or AcHS-2 (10 μM, 2.5 mL) in a buffer solution (0.01 M pH 7.0 phosphate buffer/EtOH = 4/1) were prepared in a quartz cuvette (1 cm × 1 cm). Various 250 mM analytes were prepared in pH 7.0 phosphate buffer, and a 10 μL of the analyte was added to sample. Water for sample preparation was purified with a Millipore system. All pH values were measured on a pH meter. The fluorescence quantum yields (Φ_F) of probes and compound **3** and **4** were determined in spectroscopic-grade solvents. The optical density of the dilute solution of all compounds (the references AcHS-1 and AcHS-2 and compounds **3** and **4**) was around 0.05 at the excitation wavelength, using fluorescein (Φ_f = 0.90 in 0.1 N NaOH)[25] solution and quinine sulfate (Φ_f = 0.54 in 0.1 N H_2SO_4)[26] as references at excitation wavelengths of 436 and 370 nm, respectively.

Measurements of Two-Photon Absorption Cross Section (δ). Two-photon absorption (TPA) experiments were carried out on the open-aperture Z-scan setup[27] using a femtosecond laser with a pulse duration of 140 fs and 80 MHz repetition rate. The thermal heating of the sample with high repetition-rate laser pulse was removed by the use of a mechanical chopper running at 1 kHz.[28] Nonlinear absorption coefficient β was measured by the open-aperture Z-scan technique. For the open aperture, the normalized transmittance as a function of the position along the z axis can be written as eq 1

$$Tz = \sum_{m=0}^{\infty} \frac{[-q(z)]^m}{(m+1)^{3/2}}, \text{ where } q(z) = \frac{\beta I_0 L_{eff}}{[1 + (z/z_0)^2]\alpha} \quad (1)$$

where I_0 is the input intensity at the focus $z = 0$, L is the sample length, α is the linear absorption coefficien, and β is the two-photon absorption coefficient. $z_0 = \pi\omega_0^2/\lambda$ is the Rayleigh diffraction length, and ω_0 is the radius of beam at focus. Thus, once an open-aperture Z-scan is performed, the nonlinear absorption coefficient β can be unambiguously deduced. Furthermore, the molecular TPA cross-section (σ) could be determined by using the following relationship[29]

$$\delta = (h\upsilon\beta \times 10^{-3})/(N_A d) \quad (2)$$

where h is the Planck's constant, υ is the frequency of input intensity, N_A is the Avogadro constant, and d is the concentration of the sample.

Determination of Detection Limits. The detection limit was calculated on the basis of the method reported in the literature.[30] The fluorescence emission spectra of probes were measured three times and the standard deviation of a blank measurement was achieved. The ratio of fluorescence intensity at F_{530}/F_{465} vs the concentration of Na_2S was plotted. The detection limit was calculated by using the equation detection limit = $3N/k$, where N is the standard deviation of the blank measurement k is the slope of the plot.

Cell Cultures and MTT Assays. MCF-7 cells were seeded in DMEM (Dulbecco's modified Eagle's medium) supplemented with 10% FBS (fetal bovine serum) in an atmosphere of 5% CO_2 and 95% air at 37 °C. Before the experiment, the cells well placed in a 96-well plate, followed by addition of various concentrations of probes. The final concentrations of probes vary from 0 to 20 μM. The cells were then incubated at 37 °C in an atmosphere of 5% CO_2 and 95% air for 24 h, followed by MTT assays (n = 4).

Cell-Imaging Experiments. MCF-7 cells cultured under the above condition were employed for cell-imaging experiments. The imaging of MCF-7 cells was performed by a laser scanning confocal fluorescence microscope (Zeiss LSM 510 Meta NLO). The cells were treated initially with 5 μM AcHS-2 for 1 h. Then, Na_2S (0.5 mM) was added to the incubation medium, and the cells were incubated for 1 h. The excitation wavelength was 375 or 405 nm and 750 or 805 nm for one-photon and two-photon assays, respectively. Fluorescence signals were collected from the blue channel (420–550 nm) and the green channel (500–640 nm), respectively.

The colocalization experiment was carried out at the monoemission mode. MCF-7 cells were stained by AcHS-2 (5 μM, 1 h) and MitoTracker Red CMXRos (0.5 μM, 30 min) or MitoTracker Deep Red FM (1 μM, 30 min) in sequence. The images for AcHS-2 were collected with band paths of 408–500 nm for cells stained by only AcHS-2 or 500–650 nm for cells stained by AcHS-2 and Na_2S in succession, while the images for two mitochondria dyes were collected with a band path of 600–705 nm or 665–750 nm upon excitation at 578 or 633 nm, respectively.

dx.doi.org/10.1021/jo5014838 | J. Org. Chem. XXXX, XXX, XXX–XXX

Materials. Unless stated otherwise, all chemical regents were purchased from commercial sources and used without further purification. Solvents of technical quality were distilled prior to use. Water for preparation of solutions was purified with a Millipore water system.

Synthesis of 4-Azidophenylmethanol (5).[18] 4-Azidophenylmethyl bromide (1.3 g, 0.6 mmol) was suspended in water (5 mL). Under nitrogen atmosphere, the mixture was stirred overnight at 90 °C and then cooled at room temperature and extracted with ethyl acetate. The organic phase was dried with anhydrous Na_2SO_4 and concentrated to dryness, the residue was purified using flash chromatography (EtOAc/petroleum ether, 1:4 v/v), and **5** was obtained as a yellow oil (455 mg, 50%): ^{1}H NMR ($CDCl_3$, 400 MHz) δ 7.35 (d, J = 8.1 Hz, 2H), 7.02 (d, J = 8.1 Hz, 2H), 4.67 (s, 2H) ppm.

Synthesis of *N*-*n*-Butyl-4-nitro-1,8-naphthalimide (6a).[20] *n*-Butylamine (200 μL, 1.6 mmol) was quickly added to a cloudy solution of 4-nitro-1,8-naphthalic anhydride[19] (340 mg, 1.4 mmol) in ethanol (7 mL). After being refluxed for 6 h under N_2, the reaction was allowed to cool to room temperature, filtered, and washed with cool ethanol (2 mL). The residue was purified using flash chromatography (EtOAc/petroleum ether, 1:10 v/v), and compound **6a** was obtained as a pale yellow solid (180 mg, 43%): ^{1}H NMR ($CDCl_3$, 400 MHz) δ 8.85 (dd, J = 8.7 Hz, J = 1.0 Hz, 1H), 8.74 (dd, J = 7.3 Hz, J = 1.0 Hz, 1H), 8.70 (d, J = 8.0 Hz, 1H), 8.41(d, J = 8.0 Hz, 1H), 7.98 (dd, J = 8.7 Hz, J = 7.3 Hz, 1H), 4.20 (t, J = 7.5 Hz, 2H), 1.72 (m, 2H), 1.46 (m, 2H), 0.99 (t, J = 7.3 Hz, 3H) ppm.

Synthesis of *N*-*n*-Butyl-4-amido-1,8-naphthalimide (3).[20] A stirred cloudy solution of **6a** (140 mg, 0.47 mmol) in ethanol (5 mL) was added dropwise to the solution of $SnCl_2{\cdot}2H_2O$ (677 mg, 3 mmol) in concentrated hydrochloric acid (1 mL) at room temperature for 15 min. The reaction was quenched with aqueous 10% Na_2CO_3 and filtered. After being washed with water (3 × 10 mL), the residue was dried in vacuo to afford compound **3** (98 mg, 78%): ^{1}H NMR (DMSO-d_6, 400 MHz) δ 8.61 (d, J = 8.4 Hz, 1H), 8.42 (d, J = 7.3 Hz, 1H), 8.18−8.20 (m, 1H), 7.43−7.67 (m, 1H), 7.43 (s, 2H), 6.84 (d, J = 8.4 Hz, 1H), 4.00 (t, J = 7.2 Hz, 2H), 1.54−1.62 (m, 2H), 1.28−1.38 (m, 2H), 0.93 (t, J = 7.6 Hz, 3H) ppm; ^{13}C NMR (DMSO-d_6, 75 MHz) δ 13.7, 19.8, 29.8, 40.0, 107.5, 108.1, 119.3, 121.8, 123.9, 129.2, 129.6, 130.9, 133.9, 152.6, 162.9, 163.7; IR (Nujol) $\bar{\nu}$ 3431 (s), 3355 (s), 2954 (m), 1636 (s), 1576 (s), 2372 (s), 771 cm^{-1}(s); UV/vis (pH 7.0 PBS buffer) λ_{max} (ε) 435 nm (12000 mol^{-1} dm^3 cm^{-1}); FTMS (ESI) calcd for $C_{16}H_{17}N_2O_2$ [M$^+$] 269.1284, found 269.1281.

Synthesis of AcHS-1. A mixture of **3** (134 mg, 0.5 mmol) and DMAP (192 mg, 1.50 mmol) in toluene (7.5 mL) was added dropwise to a solution of triphosgene (152 mg, 0.5 mmol) in toluene. The resulting solution was heated to reflux for 3 h. After being cooled to room temperature, the reaction mixture was diluted with CH_2Cl_2 (6 mL) and filtered. To the filtrate was added **5** (100 mg, 0.55 mmol), and the solution was stirred at room temperature for 3 h. The reaction was then concentrated and purified by flash column chromatography (EtOAc/petroleum ether, 1:2 v/v) to afford AcHS-1 as a pale yellow solid (15 mg, 6.8%): ^{1}H NMR (DMSO-d_6, 400 MHz) δ 8.56 (d, J = 8.0 Hz, 1H), 8.52 (d, J = 8.8 Hz, 1H), 8.47 (d, J = 8.4 Hz, 1H), 7.83 (t, J = 8.0 Hz, 1H), 7.64 (d, J = 8.4 Hz, 2H), 7.45 (d, J = 8.4 Hz, 1H), 7.21 (d, J = 8.4 Hz, 2H), 5.48 (s, 2H), 4.04 (t, J = 7.4 Hz, 2H), 1.61 (m, 2H), 1.35 (m, 2H), 0.94 (t, J = 7.4 Hz, 3H) ppm; ^{13}C NMR (DMSO-d_6, 75 MHz) δ 13.7, 19.8, 29.6, 40.0, 66.0, 117.1, 118.1, 119.2, 122.2, 123.8, 126.3, 128.3, 129.2, 130.2, 130.9, 131.6, 133.1, 139.3, 140.6, 153.9, 162.9, 163.4; IR (Nujol) $\bar{\nu}$ 3294 (s), 2959 (s), 2115 (m), 1692 (s), 1650 (s), 1538 (s), 1248 (s), 772 (s) cm^{-1}; UV/vis (pH 7.0 PBS buffer) λ_{max} (ε) 370 nm (13400 mol^{-1} dm^3 cm^{-1}); FTMS (ESI) calcd for $C_{24}H_{22}N_5O_4$ [M$^+$] 444.1666, found 444.1664.

Synthesis of *N*-(2-Hydroxyethyl)-4-nitro-1,8-naphthalimide (6b).[21] Aminoethanol (80 μL, 1.2 mmol) was quickly added to a cloudy solution of 4-nitro-1, 8-naphthalic anhydride (243 mg, 1.0 mmol) in 1.4-dioxane (7 mL). After being refluxed for 4 h under N_2, the reaction mixture was allowed to cool to room temperature and concentrated. The residue was purified using flash chromatography (EtOAc/petroleum ether, 4:1 v/v), and **6b** was obtained as a pale yellow solid (130 mg, 45%): ^{1}H NMR ($CDCl_3$, 400 MHz) δ 8.77−8.87 (m, 1H), 8.75−8.76 (m, 1H), 8.71 (d, J = 8.0 Hz, 1H), 8.42 (t, J = 8.0 Hz, 1H), 7.98−8.02 (m, 1H), 4.47 (t, J = 5.4 Hz, 2H), 3.99−4.02(m, 2H).

Synthesis of *N*-(2-Hydroxyethyl)-4-amido-1,8-naphthalimide (4).[21] The preparation process was the same as that used for compound **3** (88%): ^{1}H NMR (DMSO-d_6, 300 MHz) δ 8.61 (d, J = 8.4 Hz, 1H), 8.42 (d, J = 7.2 Hz, 1H), 8.19 (d, J = 7.2 Hz, 1H), 7.65 (t, J = 7.8 Hz, 1H), 7.43 (s, 2H), 6.84 (d, J = 8.4 Hz, 1H), 4.79 (s, 1H), 4.12 (t, J = 6.5 Hz, 2H), 3.58 (d, J = 5.4 Hz, 2H); ^{13}C NMR (DMSO-d_6, 75 MHz) δ 41.3, 57.9, 107.6, 108.1, 119.3, 121.8, 123.9, 129.2, 129.7, 130.9, 133.9, 152.6, 163.0, 163.9; IR (Nujol) $\bar{\nu}$ 3439 (s), 3352 (s), 3251 (s), 2958 (s), 1632 (m), 1650 (s), 1586 (s), 1380 (s), 774 (s) cm^{-1}; UV/vis (pH 7.0 PBS buffer) λ_{max} (ε) 436 nm (11800 mol^{-1} dm^3 cm^{-1}); FTMS (ESI) calcd for $C_{14}H_{13}N_2O_3$ [M$^+$] 257.0921, found 257.0919.

Synthesis of AcHS-2. The preparation process was the same as that used for AcHS-1. The reaction mixture was purified by flash column chromatography (EtOAc/petroleum ether, 1:2 v/v) to give AcHS-2 as a pale yellow solid (12 mg, 7.0%): ^{1}H NMR ($CDCl_3$, 300 MHz) δ = 8.61−8.67 (m, 2H), 8.41 (d, J = 8.4 Hz, 1H), 8.19 (d, J = 8.4 Hz, 1H), 7.78 (t, J = 7.8 Hz, 1H), 7.45−7.50 (m, 3H), 7.07 (d, J = 8.4 Hz, 2H), 5.27 (s, 2H), 4.56 (t, J = 6.8 Hz, 2H), 3.84 (t, J = 6.8 Hz, 2H) ppm; ^{13}C NMR ($CDCl_3$, 75 MHz) δ 41.7, 41.4, 67.6, 117.0, 117.6, 119.5, 123.1, 123.2, 126.5,126.8,129.2, 130. 6,131.8, 132.1, 133.1, 139.4, 140.9, 153.1, 163.7, 164.3; IR (Nujol) $\bar{\nu}$ 3437 (s), 3290 (s), 3251 (s), 2923 (m), 2115 (s), 1694, (m), 1650 (s), 1538 (s), 1250 (m), 781 (s) cm^{-1}; UV/vis (pH 7.0 PBS buffer) λ_{max} (ε) 373 nm (13400 mol^{-1} dm^3 cm^{-1}); TOF-MS (ES$^+$) calcd for $C_{22}H_{18}N_5O_5$ [M$^+$] 432.1308, found 432.1306.

■ ASSOCIATED CONTENT

Ⓢ Supporting Information

Data for detection limits, stability of probes and confocal fluorescence images of cells, and NMR spectra of related compounds. This material is available free of charge via the Internet at http://pubs.acs.org.

■ AUTHOR INFORMATION

Corresponding Author

*E-mail: qhsong@ustc.edu.cn. Fax: (+86) 0551-63601592. Tel: (+86) 0551-63607992.

Notes

The authors declare no competing financial interest.

■ ACKNOWLEDGMENTS

We are grateful for financial support from the National Natural Science Foundation of China (Grant No. 21272224) and the Science Foundation of Anhui Province (128085MB19), facility support from Prof. Jun Wang's laboratory at USTC for cell culture, and Prof. Hongping Zhou of Anhui University for measurements of two-photon excitation spectra of two probes and their sensing products (**3** and **4**).

■ REFERENCES

(1) (a) Li, L.; Rose, P.; Moore, P. K. *Annu. Rev. Pharmacol. Toxicol.* **2011**, *51*, 169−187. (b) Krishnan, N.; Fu, C.; Pappin, D. J.; Tonks, N. K. *Sci. Signal.* **2011**, *4*, ra86.

(2) (a) Ishigami, M.; Hiraki, K.; Umemura, K. Y.; Ishii, O. K.; Kimura, H. *Antioxid Redox Signal.* **2009**, *11*, 205−214. (b) Benavides, G. A.; Squadrito, G. L.; Mills, R. W.; Patel, H. D.; Isbell, T. S.; Patel, R. P.; Darley-Usmar, V. M.; Doeller, J. E.; Kraus, D. W. *Proc. Natl. Acad. Sci. U.S.A.* **2007**, *104*, 17977−17982. (c) Singh, S.; Banerjee, R. *Biochim. Biophys. Acta* **2011**, *1814*, 1518−1527.

(3) Kamoun, P. *Amino Acids.* **2004**, *26*, 243−254.

(4) Szabó, C. *Nat. Rev. Drug. Discovery* **2007**, *6*, 917−935.

(5) Kabil, O.; Banerjee, R. *J. Biol. Chem.* **2010**, *285*, 21903−21907.
(6) (a) Shibuya, N.; Tanaka, M.; Yoshida, M.; Ogasawara, Y.; Togawa, T.; Ishii, K.; Kimura, H. *Antioxid. Redox Signaling* **2009**, *11*, 703−714. (b) Kimura, Y.; Goto, Y.; Kimura, H. *Antioxid. Redox Signaling* **2010**, *12*, 1−13.
(7) (a) Mari, M.; Morales, A.; Colell, A.; Garcia-Ruiz, C.; Fernandez-Checa, J. C. *Antioxid. Redox Signaling* **2009**, *11*, 2685−2700. (b) Cheng, W. Y.; Tong, H.; Miller, E. W.; Chang, C. J.; Remington, J.; Zucker, R. M.; Bromberg, P. A.; Samet, J. M.; Hofer, T. P. *Environ. Health Perspect.* **2010**, *118*, 902−908.
(8) (a) Pun, P. B. L.; Lu, J.; Kan, E. M.; Moochhala, S. *Mitochondrion* **2010**, *10*, 83−93. (b) Fu, M.; Zhang, W.; Wu, L.; Yang, G.; Li, H.; Wang, R. *Proc. Natl. Acad. Sci. U.S.A.* **2012**, *109*, 2943−2948.
(9) (a) Zhao, W.; Zhang, J.; Lu, Y.; Wang, R. *EMBO J.* **2001**, *20*, 6008−6016. (b) Wang, R. *FASEB J.* **2002**, *16*, 1792−1798. (c) Kabil, O.; Banerjee, R. *J. Biol.chem.* **2010**, *285*, 21903−21907. (d) Lavu, M.; Bhushan, S.; Lefer, D. J. *Clin. Sci. (London)* **2011**, *120*, 219−229. (e) Olson, K. R. *Am. J. Physiol.* **2011**, *301*, R297−R312.
(10) For reviews, see: (a) Peng, H.; Chen, W.; Burroughs, S.; Wang, B. *Curr. Org. Chem.* **2013**, *17*, 641−653. (b) Kumar, N.; Bhalla, V.; Kumar, M. *Coord. Chem. Rev.* **2013**, *257*, 2335−2341. (c) Lin, V. S.; Chang, C. J. *Curr. Opin. Chem. Biol.* **2012**, *16*, 595−601. (d) Chan, J. S.; Dodani, C.; Chang, C. J. *Nat. Chem.* **2012**, *4*, 973−984.
(11) (a) Lippert, A. R.; New, E. J.; Chang, C. J. *J. Am. Chem. Soc.* **2011**, *133*, 10078−10080. (b) Peng, H.; Cheng, Y.; Dai, C.; King, A. L.; Predemore, B. L.; Lefer, D. J.; Wang, B. *Angew. Chem., Int. Ed.* **2011**, *50*, 9672−9675. (c) Chen, S.; Chen, Z. J.; Ren, W.; Ai, H.-W. *J. Am. Chem. Soc.* **2012**, *134*, 9589−9592. (d) Yu, F.; Li, P.; Song, P.; Wang, B.; Zhao, J.; Han, K. *Chem. Commun.* **2012**, *48*, 2852−2854. (e) Montoya, L. A.; Pluth, M. D. *Chem. Commun.* **2012**, *48*, 4767−4769. (f) Das, S. K.; Lim, C. S.; Yang, S. Y.; Han, J. H.; Cho, B. R. *Chem. Commun.* **2012**, *48*, 8395−8397. (g) Xuan, W.; Pan, R.; Cao, Y.; Liu, K.; Wang, W. *Chem. Commun.* **2012**, *48*, 10669−10671. (h) Wu, Z.; Li, Z.; Yang, L.; Han, J.; Han, S. *Chem. Commun.* **2012**, *48*, 10120−10122. (i) Wu, M.; Li, K.; Hou, J.; Huang, Z.; Yu, X. *Org. Biomol. Chem.* **2012**, *10*, 8342−8347. (j) Wan, Q.; Song, Y.; Li, Z.; Gao, X.; Ma, H. *Chem. Commun.* **2013**, *49*, 502−504. (k) Sun, W.; Fan, J.; Hu, C.; Zhang, H.; Xiong, X.; Wang, J.; Cui, S.; Sun, S.; Peng, X. *Chem. Commun.* **2013**, *49*, 3890−3892. (l) Bae, S. K.; Heo, C. H.; Choi, D. J.; Sen, D. E.; Joe, H.; Cho, B. R.; Kim, H. M. *J. Am. Chem. Soc.* **2013**, *135*, 9915−9923. (m) Bailey, T. S.; D. Pluth, M. *J. Am. Chem. Soc.* **2013**, *135*, 16697−16704. (n) Zhu, D.; Li, G.; Xue, L.; Jiang, H. *Org. Biomol. Chem.* **2013**, *11*, 4577−4580. (o) Chen, B.; Li, W.; Lv, C.; Zhao, M.; Jin, H.; Jin, H.; Du, J.; Zhang, L.; Tang, X. *Analyst* **2013**, *138*, 946−951. (p) Mao, G.; Wei, T.; Wang, X.; Huan, S.; Lu, D.; Zhang, J.; Zhang, X.; Tan, W.; Shen, G.; Yu, R. *Anal. Chem.* **2013**, *85*, 7875−7881. (q) Li, W.; Sun, W.; Yu, X.; Du, L.; Li, M. *J. Fluoresc.* **2013**, *23*, 181−186. (r) Zhang, H. T.; Wang, P.; Chen, G. C.; Cheung, H.-Y.; Sun, H. Y. *Tetrahedron Lett.* **2013**, *54*, 4826−4829. (s) Zheng, Y.; Zhao, M.; Qiao, Q. L.; Liu, H. Y.; Lang, H. J.; Xu, Z. C. *Dyes Pigments.* **2013**, *98*, 367−371. (t) Chen, T.; Zheng, Y.; Xu, Z. C.; Zhao, M.; Xu, Y. G.; Cui, J. N. *Tetrahedron Lett.* **2013**, *54*, 2980−2892. (u) Reja, S. I.; Kumar, N.; Sachdeva, R.; Bhalla, V.; Kumar, M. *RSC Adv.* **2013**, *3*, 17770−17774.
(12) Recent samples: (a) Wang, X.; Sun, J.; Zhang, W.; Ma, X.; Lv, J.; Tang, B. *Chem. Sci.* **2013**, *4*, 2551−2556. (b) Chen, Y.; Zhu, C.; Yang, Z.; Chen, J.; He, Y.; Jiao, Y.; He, W.; Qiu, L.; Cen, J.; Guo, Z. *Angew. Chem., Int. Ed.* **2013**, *52*, 1688−1691. (c) Liu, J.; Sun, Y.; Zhang, J.; Yang, T.; Cao, J.; Zhang, L.; Guo, W. *Chem.—Eur. J.* **2013**, *19*, 4717−4722. (d) Li, X.; Zhang, S.; Cao, J.; Xie, N.; Liu, T.; Yang, B.; He, Q.; Hu, Y. *Chem. Commun.* **2013**, *49*, 8656−6558. (e) Liu, T.; Xu, Z.; Spring, D. R.; Cui, J. *Org. Lett.* **2013**, *15*, 2310−2313. (f) Montoya, L. A.; Pearce, T. F.; Hansen, R. J.; Zakharov, L. N.; Plut, M. D. *J. Org. Chem.* **2013**, *78*, 6050−6064. (g) Chen, X.; Wu, S.; Han, J.; Han, S. *Biol. Med. Chem. Lett.* **2013**, *23*, 5295−5299. (h) Qian, Y.; Yang, B.; Shen, Y.; Du, Q.; Lin, L.; Lin, J.; Zhu, H. *Sens. Actuators B* **2013**, *182*, 498−503. (i) Wang, J. L.; Lin, W. Y.; Li, W. L. *Biomaterials* **2013**, *34*, 7429−7436. (j) Zhang, J. Y.; Sun, Y. Q.; Liu, J.; Shi, Y. W.; Guo, W. *Chem. Commun.* **2013**, *49*, 11305−11307. (k) Liu, T. Y.; Zhang, X. F.; Qiao, Q. L.; Zou, C. Y.; Feng, L.; Cui, J. N.; Xu, Z. C. *Dyes Pigments* **2013**, *99*, 537−542.
(13) Recent samples: (a) Sasakura, K.; Hanaoka, K.; Shibuya, N.; Mikami, Y.; Kimura, Y.; Komatsu, T.; Ueno, T.; Terai, T.; Kimura, H.; Nagano, T. *J. Am. Chem. Soc.* **2011**, *133*, 18003−180035. (b) Qu, X.; Li, C.; Chen, H.; Mack, J.; Guo, Z.; Shen, Z. *Chem. Commun.* **2013**, *49*, 7510−7512.
(14) (a) Wang, B. S.; Li, P.; Yu, F. B.; Song, P.; Sun, X. F.; Yang, S. Q.; Lou, Z. R.; Han, K. L. *Chem. Commun.* **2013**, *49*, 1014−1016. (b) Wang, B. S.; Li, P.; Yu, F. B.; Chen, J. S.; Qu, Z. J.; Han, K. L. *Chem. Commun.* **2013**, *49*, 5790−5792. (c) Lina, V. S.; Lippert, A. R.; Chang, C. J. *PNAS USA* **2013**, *110*, 7131−7135. (d) Wei, L.; Yi, L.; Song, F. B.; Wei, C.; Wang, B. F.; Xi, Z. *Sci. Rep.* **2014**, *4*, 4521. (e) Yuan, L.; Zuo, Q.-P. *Chem.—Asian J.* **2014**, *9*, 1544−1549.
(15) Qian, X.; Xiao, Y.; Xu, Y.; Guo, X.; Qian, J.; Zhu, W. *Chem. Commun.* **2010**, *46*, 6418−6436.
(16) Zhang, J. F.; Lim, C. S.; Bhuniya, S.; Cho, B. R.; Kim, J. S. *Org. Lett.* **2011**, *13*, 1190−1193.
(17) Srikun, D.; Miller, E. W.; Domaille, D. W.; Chang, C. J. *J. Am. Chem. Soc.* **2008**, *130*, 4596−4597.
(18) Robinson, A.-M.; Evers, E. L.; Griffin, R. J.; Irwin, W. J. *J. Pharm. Pharmacol.* **1988**, *40*, 61P.
(19) (a) Cava, M. P.; Merkel, K. E.; Schlessinger, R. H. *Tetrabedron* **1965**, *21*, 3059−3064. (b) Dong, M.; Wang, Y. W.; Peng, Y. *Org. Lett.* **2010**, *12*, 5310−5313.
(20) Wu, J.; Huang, R.; Wang, C. C.; Liu, W. T.; Wang, J. Q.; Weng, X. C.; Tian, T.; Zhou, X. *Org. Biomol. Chem.* **2013**, *11*, 580−585.
(21) Zhang, J. F.; Kim, S.; Han, J. H.; Lee, S.-J.; Pradhan, T.; Cao, Q. Y.; Lee, S. J.; Kang, C.; Kim, J. S. *Org. Lett.* **2011**, *13*, 5294−5297 and references therein.
(22) Perrin, D. D. *Ionization Constants of Inorganic Acids and Bases in Aqueous Solution*, 2nd ed.; Pergamon: Oxford, 1982.
(23) (a) Dombkowski, R. A.; Russell, M. J.; Olson, K. R. *Am. J. Physiol.* **2004**, *286*, R678−R685. (b) Hughes, M. N.; Centelles, M. N.; Moore, K. P. *Free Radical Biol. Med.* **2009**, *47*, 1346−1353.
(24) *A Guide to Fluorescent Probes and Labeling Technologies*, 11th ed.; Johnson, I., Spence, M. T. Z., Eds.; The Molecular Probes: Eugene, OR, 2010.
(25) Demas, J. N.; Crosby, J. A. *J. Phys. Chem.* **1971**, *73*, 991−1024.
(26) Dawson, W. R.; Windsor, M. W. *J. Phys. Chem.* **1968**, *72*, 3251−3260.
(27) Ji, Z.; Li, Y.; Pritchett, T. M.; Makarov, N. S.; Haley, J. E.; Li, Z.; Drobizhev, M.; Rebane, A.; Sun, W. *Chem.—Eur. J.* **2011**, *17*, 2479−2491.
(28) Zheng, Q.; He, G. S.; Prasad, P. N. *J. Mater. Chem.* **2005**, *15*, 579−587.
(29) Li, D. M.; Zhang, Q.; Wang, P.; Wu, J. Y.; Kan, Y. H.; Tian, Y. P.; Zhou, H. P.; Yang, J. X.; Tao, X. T.; Jiang, M. H. *Dalton Trans.* **2011**, *40*, 8170−8178.
(30) Fan, J.; Sun, W.; Hu, M.; Cao, J.; Cheng, G.; Dong, H.; Song, K.; Liu, Y.; Sun, S.; Peng, X. *Chem. Commun.* **2012**, *48*, 8117−8119.